Comparative Study of Free Energies of Solvation of Phenylimidazole Inhibitors of Cytochrome P450*cam* by Free Energy Simulation, AMSOL, and Poisson Boltzmann Methods

DAN HARRIS* and GILDA LOEW

Molecular Research Institute, 845 Page Mill Road, Palo Alto, California 94304

Received 8 November 1994; accepted 10 May 1995

ABSTRACT

Free energies of solvation of phenylimidazole inhibitors of cytochrome P450*cam* were determined using (1) free energy simulation, (2) AMSOL-SM2 semiempirical methods, and (3) Poisson-Boltzmann methods. The goals of this study were threefold: (1) to compare the results obtained from the three different methods, (2) to investigate the effect of inclusion of intraperturbed group interactions on free energy simulation estimates of solvation free energy differences, and (3) to investigate to what extent differences in free energies of solvation among three of these inhibitors could account for observed differences in their enzyme binding free energies. In general, relative solvation free energies obtained from the free energy simulations and AMSOL-SM2 methods give comparable results (i.e., the same rank ordering and similar quantitative results, differing significantly from results obtained using Poisson-Boltzmann methods). The free energy simulation studies suggest that the neglect of intraperturbed group interactions had little effect on rank order of free energies of solvation of the polar phenylimidazoles. The relative desolvation free energies of the three inhibitors of P450*cam*—1-phenylimidazole (1-PI), 2-phenylimidazole (2-PI), and 4-phenylimidazole (4-PI)—with known enzyme bound X-ray structures parallel that of their known binding affinities and could account for most of the differences in the free energies of binding of these three inhibitors to P450*cam*. The origin of the difference of the free energies of solution of these three inhibitors is primarily the additional interaction between solvent and N—H group in the imidazole ring of 2- and 4-phenylimidazole that is absent in the

* Author to whom all correspondence should be addressed.

Journal of Computational Chemistry, Vol. 17, No. 3, 273–288 (1996)

CCC 0192-8651 / 96 / 030273-16

1-phenylimidazole isomer. This hypothesis is substantiated by a second comparison of the relative solvation free energies of 4-phenylimidazole with its methylated derivative, 3-methyl-4-phenylimidazole, also lacking an N—H group.

Introduction

Cytochrome P450*cam* is a member of a ubiquitous family of metabolizing heme enzymes with functions varying from steroid biosynthesis to oxidative metabolism of xenobiotics. P450*cam*, a water-soluble P450 camphor hydroxylase from the bacteria *pseudomonas putida*, was the first member of this family to have its crystal structure solved.[1] Subsequently, structures of P450*cam* complexes with three phenylimidazole isomers and metapyrone inhibitors were reported by the same laboratory.[2] The binding constants of these same inhibitors had previously been characterized by Libscomb employing electron paramagnetic resonance (EPR) spectroscopy.[3]

Figure 1a shows the structures of the 1-phenylimidazole (1PI), 2-phenylimidazole (2-PI), and 4-phenylimidazole (4-PI) isomers, and Figure 2 shows their orientation in the binding pocket of P450*cam*, from the crystal structures of these complexes. As seen in Figure 2, both 1- and 4-phenyl-

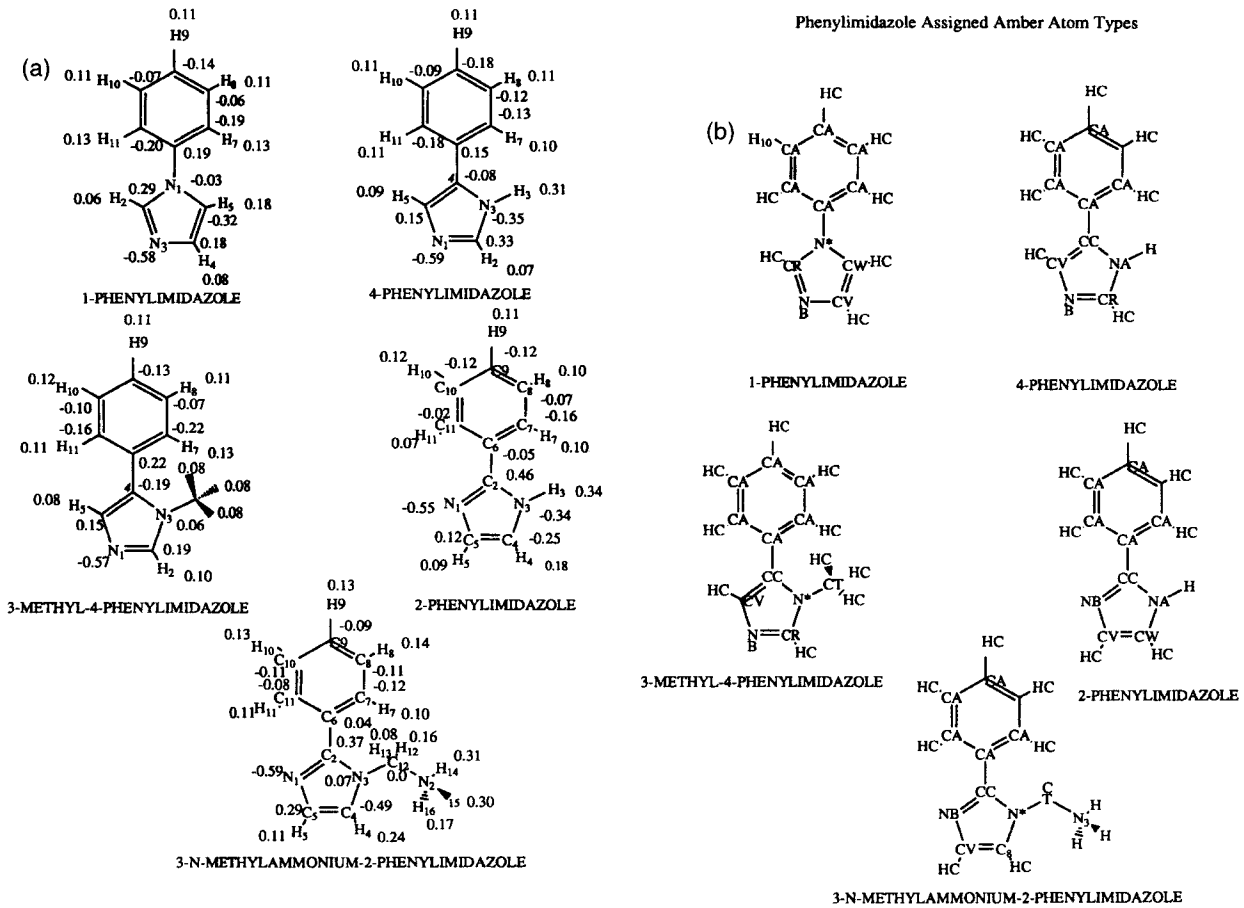

FIGURE 1. (a) The structures of 1-phenylimidazole, 2-phenylimidazole, 4-phenylimidazole, 3-methyl-4-phenylimidazole, and 3-methylammonium-2-phenylimidazole with CHELPG atom-centered charges reproducing their molecular electrostatic potential surfaces and assigned atom names. (b) The structures of the phenylimidazole studied with their superimposed AMBER atom types.

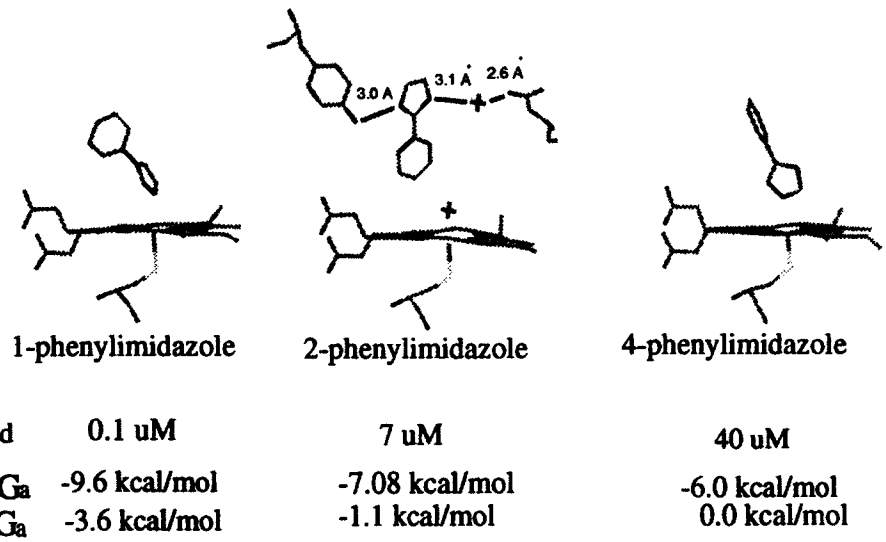

FIGURE 2. The binding modes of 1-phenylimidazole, 2-phenylimidazole, and 4-phenylimidazole above the heme in their respective inhibitor bound cytochrome P450*cam* crystal structures (ref. 2). As indicated, only residues indicated in the crystal structure to be hydrogen bonding directly to the inhibitors are shown (as in the case of 2-phenylimidazole); all other surrounding residues are not shown. The experimental inhibitor P450*cam* binding affinity constants are also given (ref. 3).

imidazoles bind to P450*cam* as ligands to the heme iron via their imidazole nitrogen, and neither have specific polar interactions in the binding site; while the 2-phenylimidazole inhibitor is not a heme iron ligand and binds in an orientation such that it has hydrogen bonding donor and acceptor partners for both its imidazole N and NH groups. Specifically, the imidazole N is hydrogen bonded to Y96 and the NH group to an adjacent water molecule, which in turn is hydrogen bonded to T185 and Asp 251. A water molecule is the sixth ligand of the heme iron in this inhibitor bound crystal structure.

In a previous study we reported full protein molecular dynamics (MD) studies of these enzyme-bound inhibitors that led to MD-averaged interaction energies in the order of 4-PI > 1-PI > 2-PI (i.e., −43, −41, and −38 kcal/mol, respectively). These MD-average interaction energies do not, however, explain the relative ordering of their observed binding affinities given in Figure 2: 1-PI > 2-PI > 4-PI (ref. 4) since they do not include effects such as entropy changes and desolvation free energetics, which are potentially important determinants of the relative free energies of binding of such inhibitors.

As illustrated in the following thermodynamic cycle,

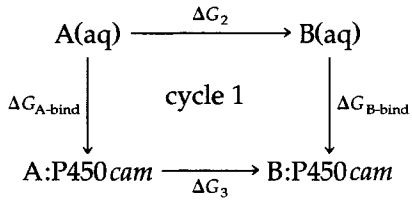

$$\Delta\Delta G\text{bind} = \Delta G_{\text{B-bind}} - \Delta G_{A\text{-}bind} = \Delta G_3 - \Delta G_2$$

the measured difference in the free energies of binding of two inhibitors, A and B, ($\Delta G_{\text{B-bind}} - \Delta G_{\text{A-bind}}$) is equal to the difference in their free energies of transformation bound to the enzyme and in solution ($\Delta G_3 - \Delta G_2$). The experimental results shown in Figure 2 indicate that the experimental difference in free energy of binding of the 4- and 1-phenylimidazole isomers to P450*cam* is -3.6 kcal mol^{-1} while the difference in free energy of binding of the 4- and 2-phenylimidazole isomers is -1.1 kcal mol^{-1}. It is surprising that it is 1-phenylimidazole, with the least potential for

hydrogen bonding to the binding site residues of P450*cam*, that has the highest affinity (i.e., the most negative free energy of binding).

In this work we have assessed the possible role of differences in solvation energy in the measured differences in free energy of these three inhibitors by calculating and comparing the free energies of solvation of 1-, 2-, and 4-phenylimidazole. These results can also be used as the first step in the complete determination of the origin of the differences in free energies of binding of these inhibitors to P450*cam* relative to solution. In the absence of experimental data for solvation free energies of these inhibitors, we have calculated the relative solvation energies using three different theoretical methods.

In the first approach, relative free energies of desolvation of each pair of inhibitor (A and B) were calculated using free energy simulations and the following thermodynamic cycle 2:

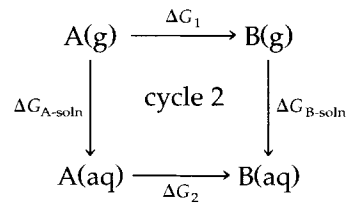

$$\Delta\Delta G\text{solv} = \Delta G_{\text{B-soln}} - \Delta G_{\text{A-soln}} = \Delta G_2 - \Delta G_1$$

to determine their relative free energies of transformation in solution relative to the gas phase ($\Delta G_2 - \Delta G_1$). The ability of free energy simulations to make accurate predictions of relative solvation free energies has been demonstrated by many groups, as noted in a recent review of this methodology.[5] The second method used was the AMSOL-AM1-SM2 model, which has also been successful in describing the solvation free energies of numerous molecular systems using a combination of semiempirical quantum mechanical methods and continuum reaction field descriptions of solvent.[6] Finally, the continuum electrostatic approach in the form of the Poisson-Boltzmann equation can be a useful method for calculating relative solvation free energies when entropic contributions are relatively unimportant. Although the quantity calculated using this method is not properly a solvation free energy and in fact only includes electrostatic energetic contributions, we will refer to it as a free energy estimate.

We have also performed these calculations for 3-methyl-4-phenylimidazole and 3-methylammonium-2-phenylimidazole to (1) provide support for the proposed role of the free NH group in the 4-PI compound as the origin of the differences in observed binding affinities of 1- and 4-phenylimidazole, and (2) to examine the desolvation costs of charged derivatives of phenylimidazoles. These results provide a useful comparison of three common methods for calculating solvation free energies, as well as a measure of the role of the free energy of desolvation in the known $\Delta\Delta G_{\text{binding}}$ of several inhibitors of P450*cam*.

Methods

CHARACTERIZATION OF INHIBITOR GEOMETRIES AND PARAMETER DEVELOPMENT

Geometry optimized structures of the five inhibitors studied were obtained by *ab initio* calculations using Gaussian 92[7] and a 6-31G* basis set. The charges used in AMBER 4.0[8] calculations were obtained by fitting atomic charges (a CHELPG[9] fit) to the molecular electrostatic potential surface derived from a single-point 6-31G*//6-31G* calculation. These atom-centered charges are shown in Figure 1a. In addition, Figure 1b shows the AMBER 4.0 atom types assigned to the corresponding inhibitor atoms. One additional atom type was defined and added (C8) to the standard AMBER 4 atom types in the case of 3-*N*-methylammonium-2-phenylimidazole (cf. Fig. 1b) and assigned parameters equivalent to the CW atom type of AMBER. The AMBER 4.0 parameterization does not include vibrational force field parameters for several of the bond, angle, and torsion combinations found in the phenylimidazoles studied (e.g., for the N*—CA, CA—N*—CW, or CA—CA—N*—CW bond, angle, and torsion values in 1-phenylimidazole), and these were imported from the force field in Quanta/CHARMM.[10†] The structures of the inhibitors were energy optimized using the SANDER module of AMBER 4,[8] which encompasses code to perform steepest descents/conjugate-gradient energy-structure minimization as well as molecular dynamics. These optimized structures were similar to those obtained from the gas phase *ab initio* calculations. The most significant qualitative differences between the molecular mechanics and *ab initio*

† Explicit information for the vibrational force field parameterization employed by the authors for the study of inhibitors in this work will be made available upon written request.

structures were small differences in the energy-minimized torsion angles between the phenyl and imidazole rings, which are not significant to the problem considered here.

FREE ENERGY SIMULATIONS

Procedures Common to All Free Energy Simulations

All free energy simulations were performed using the GIBBS module of AMBER 4, which allows calculation of relative free energies of systems from molecular dynamics simulations using either free energy perturbation of thermodynamic integration methods. The entire inhibitor was treated as the "perturbed" group. The phenylimidazole structures were immersed in a box of waters and all waters farther than 11 Å from any atom in the inhibitor were deleted. The hydrated system was energy minimized using 200 steps employing steepest descents minimization followed by an additional 2000 steps of conjugate gradient using SANDER. The system was then equilibrated for 100 ps at constant volume (or a constant pressure of ca. 1 atm by continual volume scaling) and a constant temperature of 300 K by heat bath coupling using the GIBBS module of AMBER 4. Periodic boundary conditions were employed for the mapping of solvent. The minimum-image convention was used in evaluating nonbonded interactions in conjunction with spherical truncation of the nonbonded energy terms at 10 Å.

Dummy atoms were added, where appropriate, to ensure that the topologies of the product and reactant geometries of the inhibitors were the same. For example, while none are required to simulate the interconversion of 1- and 4-phenylimidazole (cf. Fig. 1b), it is necessary to add "dummy" hydrogens to the AMBER type NB atoms of 4-phenylimidazole and 2-phenylimidazole to make their topologies equivalent, thus solving the simulation endpoint catastrophe wherein an atom perturbatively disappears or appears which can result in simulation instability. Such dummy atoms have no nonbonded terms associated with them but have finite length associated with their bonds to heavy atoms of 0.3 Å at λ endpoints where a real atom has been perturbatively transformed to a dummy atom. For example, as CV—HC in 4PI is transformed into NB—DH (DH = dummy hydrogen), the CV—HB bond length converts to the NB—DH bond length of 0.3 Å at the end of the transformation.

In all simulations except one made for comparison, the free energy perturbation method was employed using double-wide sampling (at each λ the free energies are calculated for the steps $\lambda + d\lambda$ and $\lambda - d\lambda$) and free energy was evaluated using the equation

$$G(\lambda_{i+1}) = -\mathrm{RT}\ln\langle\exp[-(\mathrm{H}(\lambda i + \Delta\lambda) - \mathrm{H}(\lambda_i))/\mathrm{RT}]\rangle_{\lambda i} \quad (1)$$

In all the free energy simulations, a constant $\Delta\lambda$ spacing of 0.02 was used with 2 ps of equilibration and 4 ps of sampling for each $\Delta\lambda$ window, resulting in simulations of 300-ps lengths. In all simulations but one (as noted in Table IIc), the integration timestep used was 0.001 ps. In all simulations, except the few made for comparison purposes, SHAKE holonomic bond length constraints were used.

Although the magnitude of the errors in the separate enthalpy, internal energy, and entropy contributions to the solvation free energies are at least an order of magnitude greater than that in the Gibbs or Helmholz free energy ($\Delta\Delta G_{\mathrm{soln}}$/$\Delta\Delta A_{\mathrm{soln}}$) values themselves, these contributions were nevertheless calculated for all but one simulation, since they provided some additional insight into these processes.

Variations in Methodologies (Conditions) used in Free Energy Simulations

Systematic variations were made in the procedures described earlier in selected cases to examine the effect of a number of specific approximations on the results of the free energy simulations. Chief among these were the following:

1. *The treatment of intraperturbed group interactions.* To investigate this effect, three types of calculations of relative free energies of solvation of one pair of inhibitors (4PI/1PI) were made.
   a. In one set of calculations, all intraperturbed group interactions are ignored. In this approximation, the $\Delta\Delta G_{\mathrm{solv}}$ or $\Delta\Delta A_{\mathrm{solv}}$ is just equal to the free energy change in the aqueous path [e.g., $\Delta\Delta G_{\mathrm{solv}} = \Delta G_{\mathrm{solv}}(\mathrm{B}) - \Delta G_{\mathrm{solv}}(\mathrm{A}) \approx \Delta G_2$ (cf. cycle 2)]. This often used approximation is based on the assumption recently called into

question[11] that the contributions to the free energies arising from intraperturbed group interactions are large, and will probably cancel when different parts of the thermodynamic cycle are combined.

b. In a second and third set of calculations, respectively, just intraperturbed nonbonded interactions and then all intraperturbed group interactions were included. In both of these approximations, the $\Delta\Delta G_{solv}$ or $\Delta\Delta A_{solv}$ is equal to the free energy change in the aqueous path minus the free energy change in the gas phase [e.g., $\Delta\Delta G_{solv} = \Delta G_{solv}(B) - \Delta G_{solv}(A) \approx \Delta G_2 - \Delta G_1$ (cf. cycle 2)].

2. *The treatment of bond length changes.* The merit of using bond length constraints in free energy simulations is an active area of concern.[11-14] To investigate this effect on free energy simulations, we have performed free energy simulations for the 4PI/1PI inhibitor pair with and without bond constraints in the approximation of ignoring intraperturbed group contributions and with all other conditions of simulation the same. For the constrained calculation, SHAKE holonomic bond length constraints were employed.

3. *Comparison of thermodynamic quantities calculated by free energy perturbation methods versus a thermodynamic integration procedure.* These two methods were compared for one case: the differences in free energies of solvation of the 4PI and 1PI inhibitor pair at constant volume, ignoring intraperturbed group contributions. In the free energy perturbation method, double-wide sampling was employed (at each λ the free energies are calculated for the steps $\lambda + d\lambda$ and $\lambda - d\lambda$), and eq. (1) was used to evaluate free energies. In the thermodynamic integration calculation, the total free energy changes were calculated using eq. (2):

$$G_1 - G_0 = \int_0^1 \langle \partial H/\partial\lambda \rangle_\lambda \, d\lambda \qquad (2)$$

wherein the integrand is determined numerically for a series of discrete points to obtain estimates of the differences in free energies of solvation for 1- and 4-phenylimidazole. The result of predictions of the free energies and less accurate enthalpy and entropy differences from these two formalisms was compared. The enthalpy and entropy relationships from the thermodynamic integration method are derived from exact integral relationships,[15] and the results will not necessarily be equal to the reported free energy. The difference between these two quantities may be taken as a crude indication of the reliability of the enthalpy/entropy values for that method. The enthalpic and entropic contributions derived from free energy perturbation are approximated from finite difference estimates of temperature derivatives[16] and are equal to the free energy estimate.

4. *Comparisons of the results from constant pressure/temperature and constant volume/temperature simulations.* These two conditions were compared for one case: the differences in free energies of solvation of the 4PI and 1PI inhibitor pair in the approximation of ignoring intraperturbed group contributions.

AMSOL-AM1-SM2 (AM1-SOLVATION MODEL 2)[17] CALCULATIONS

These calculations were performed and results were compared in two approximations: (1) with frozen inhibitor geometries taken from the 6-31G* *ab initio* geometries for the inhibitors, and (2) by allowing these initial geometries to be fully optimized in the calculations for both the gas phase and solvation model calculations. Solvation free energies for the inhibitors were obtained as the difference in the free energy plus heat of formation results from the reaction field calculation and the heat of formation from the gas phase calculation. The semiempirical basis of the method has been shown to be adequate, at the AM1 parameterized level, to be a reliable predictor of solution free energies containing second-row heteroatoms.[6,17] The AMSOL-AM1-SM2 method, like the previous AM1-SM1 method, has a modified AM1 Fock matrix which includes a generalized Born model polarization term and an accessible area term. The method has been parameterized to make estimates of the polarization/reaction field and cavity dispersion. This term, in principle, includes contributions from dispersion energy contributions upon dissolution, energetic and entropic terms associated with solvent reorganization, as well as other terms associated with pressure–volume and libra-

tional/rotational/vibrational changes upon dissolution of the solute.

The Poisson-Boltzmann calculations were performed to calculate estimates of the free energies of solution, using Delphi[18] in the following manner. First, a calculation was made employing a grid 15 Å larger than any dimension of the molecule and employing full-coulombic boundary conditions using a continuum solvent dielectric constant of 80 and of unity. Second, a calculation was made employing electrostatic-focusing boundary conditions to obtain final results for ΔG_{soln} using a grid with a border extending 10 Å beyond the molecular dimensions again at $\varepsilon = 80$ and $\varepsilon = 1$. In this methodology the ΔG_{soln} values are the direct result of calculating

$$\Delta G^{soln} = \frac{1}{2}\sum_i q_i(\phi_i^{solvent} - \phi_i^{vacuum}) \qquad (3)$$

where

q_i = the charges at each grid site i

$\phi_i = \phi_i^{total} = \phi_i^{grid} + \phi_i^{self} + \phi_i^{coul} + \phi_i^{cross}$ contributions for $\varepsilon = 1$ (vacuum) and $\varepsilon = 80$ (solvent)

ϕ_i^{self} = potential due to a charge's interaction with its own reaction field

ϕ_i^{cross} = potential due to a charge's interaction with the reaction field of other solute charge sites

ϕ_i^{coul} = potential interaction of solute charge site with other charge sites

ϕ_i^{grid} = grid base potential local to charge site I

The charges used to calculate the continuum electrostatic estimates of the free energies of solvation were the 6-31G* derived charges also used in the free energy simulation parameterization. These calculations were performed using the optimized 6-31G* phenylimidazole geometries.

Calculation of Solvent Distribution Functions around Polar Inhibitor Atoms

To obtain insight into the differences in interaction of the inhibitors with solvent that can account for the calculated differences in their free energies of solvation, the distribution function of water atoms around the N and NH imidazole atoms of

TABLE I.
Relative Thermodynamic Quantities of Inhibitor Solvation Derived from Free Energy Simulations Neglecting Intraperturbed Group Contributions.[a]

A. Results at Constant Pressure and Temperature

Inhibitor	Direction	$\Delta\Delta G_{soln}$	$\Delta\Delta H_{soln}$	$T(\Delta\Delta S_{soln})$
4-PI → 1-PI[b]	Forward	3.36		
	Reverse	−3.47		
4-PI → 1-PI	Forward	3.39	1.47	−1.92
	Reverse	−3.39	−2.52	0.87
4-PI → 1-PI[c]	Forward	3.36	4.69	−2.09

B. Results at Constant Volume and Temperature

Inhibitor	Direction	$\Delta\Delta A_{soln}$	$\Delta\Delta E_{soln}$	$T(\Delta\Delta S_{soln})$
4-PI → 1-PI[b]	Forward	3.09	−0.22	−3.31
	Reverse	−3.32	0.63	3.95
4-PI → 1-PI	Forward	2.98	+0.69	−2.30
	Reverse	−3.01	−0.80	+2.21
4-PI → 3-M4PI[b]	Forward	2.89	6.67	3.77
	Reverse	−3.35	−8.77	−5.41
2-PI → 4-PI	Forward	−0.77	+1.75	2.52
	Reverse	0.49	−2.59	−3.09

[a] All calculations were performed using free energy perturbation method [eq. (1)] using constrained solute bond lengths (SHAKE) except as noted. All calculations using TIP3P waters held rigid with SHAKE.
[b] Solute bond lengths not constrained.
[c] Thermodynamic integration used [eq. (2)].

three inhibitors 4-PI, 2-PI, and 1-PI was calculated from 120-ps molecular dynamic simulations at constant T and volume by computing

$$g(R) = \frac{\langle N(R + \Delta R)\rangle}{\rho 4\pi R^2 dR} \quad (4)$$

where $\langle N(R + \Delta R)\rangle$ is the average number of water oxygen or hydrogen atoms within a shell $R + \Delta R$ from the inhibitor atom. The denominator normalizes the distribution so that $g(R)$ is unity when the distribution of solvent atoms are at bulk density (ρ) about the inhibitor atom.

Results and Discussion

Table I, parts a and b, presents results from free energy simulations conducted in approximation of neglect of intraperturbed group interactions under a variety of conditions in order to compare the effect of these variations on estimates of relative free energies of solvation of inhibitors of cytochrome P450*cam* from free energy simulations.

Table Ia presents results of three free energy simulations for the interconversion of 1- and 4-phenylimidazole in aqueous solution at constant temperature and pressure. The forward direction in this table corresponds to the conversion of 4-phenylimidazole to 1-phenylimidazole. A comparison of the forward and reverse results in Table Ia and Figure 3 indicates little hysteresis in these calculations. Comparisons of results from the first two of these simulations illustrate the relative insensitivity of free energy results, which exclude intraperturbed bond contributions, to the presence or absence of bond length constraints for these inhibitors, since the inclusion of SHAKE constraints results in little change in the calculated $\Delta\Delta G_{soln}$. A comparison of the forward results for the first two calculations employing free energy perturbation [eq. (1)] and the third employing thermodynamic integration [eq. (2)] indicates little difference in the calculated $\Delta\Delta G_{soln}$ obtained from these different procedures. All result in a positive difference in the free energies of solution on transformation of 4-phenylimidazole into 1-phenylimidazole in aqueous solution, with a $\Delta\Delta G_{soln} \approx$

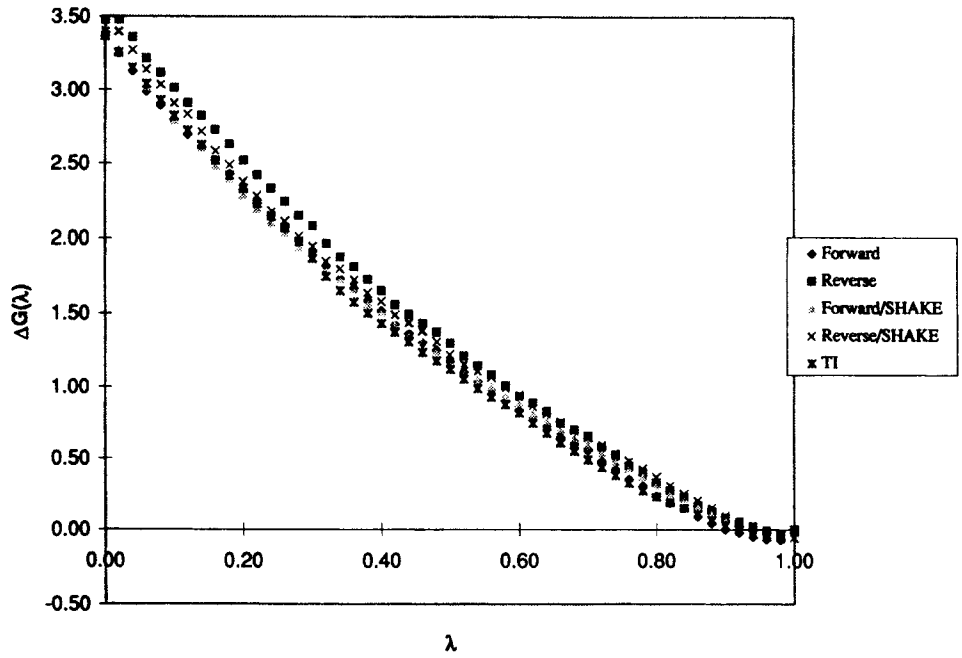

FIGURE 3. ΔG vs. λ plots for three different simulations of the transformation of 4-phenylimidazole to 1-phenylimidazole in aqueous solution at constant temperature and pressure. One (forward and reverse) is with all bond lengths held fixed at their energy-minimized values, the second is with unconstrained bond lengths (forward and reverse) both determined using free energy perturbation [eq. (1)] and a third simulation employs thermodynamic integration [eq. (2)].

$+3.4 \pm 0.1$ kcal mol^{-1}. As expected, the main differences in these two procedures are the individual calculations of the enthalpy and entropy contributions to the free energy results. The component results from the thermodynamic integration procedure are obtained independently, and the large disparity between the free energy obtained directly and by adding the contribution of the enthalpy and entropy terms is an indication of the uncertainty in these individual terms.

Table Ib gives results for the relative free-energy of solvation of 1- and 4-phenylimidazole from two free energy perturbation simulations, determined under constant volume. As for the constant pressure results, the results for $\Delta\Delta A_{soln}$ for the simulations at constant volume with and without bond length constraints are comparable. The $\Delta\Delta A_{soln}$ derived from these simulations is 3.1 ± 0.2 kcal mol^{-1}, very similar to the results obtained from constant pressure simulations.

The more favorable interaction of the 4-phenylimidazole with the aqueous solvent, as determined by the values of $\Delta\Delta G_{soln}/\Delta\Delta A_{soln}$, appears to be a direct consequence of the presence of the imidazole N—H group in 4-phenylimidazole, which is absent in the 1-phenylimidazole. To test this hypothesis, we performed simulations for another pair of compounds with and without this free N—H group by considering the mutation of 4-phenylimidazole to 3-methyl-4-phenylimidazole, simulated with bond length constraints under constant volume conditions. The free energy result for this transformation is $\Delta\Delta A_{soln} = +2.89$ kcal mol^{-1} (Table Ib), similar to those for the transformation from 4-phenylimidazole to 1-phenylimidazole, $\Delta\Delta A_{soln} = +2.98$ kcal mol^{-1}. The finding that in both comparisons, the 4-phenylimidazole with the free NH group has the more favorable free energy of solution by about the same amount, lends support to the hypothesis that the origin of this enhanced stability is the additional interactions of the NH group with solvent absent in both of the other compounds. Table Ib also gives the calculated value of the relative free energies of solvation of 2- and 4-phenylimidazole of $\Delta\Delta A$(2-PI $\rightarrow$ 4PI) $= -0.6$ kcal mol^{-1}. This smaller difference in the free energies of solvation between 2-PI and 4-PI is not surprising given the accessibility in both isomers of both N—H and N centers to solvent hydrogen bond donors and acceptors.

Summarizing the comparisons made in Table I, we see that for the systems being studied, relative free energies of solvation results are comparable for (1) constant pressure and constant volume simulations and (2) free energy perturbation and thermodynamics integration algorithms. Furthermore, they are independent of whether or not bond lengths in the perturbed group are constrained via SHAKE. Therefore, the remainder of the free energy simulations investigating the impact of including various intraperturbed group contributions to free energetics, reported in Table II, were performed using constrained bond length and constant volume conditions and employing the free energy perturbation method. Given that these calculations include intraperturbed group contributions, both the gas and aqueous solution results must be calculated to obtain the final free energy of solvation differences.

Table II presents results for the relative free energies of simulations of five phenylimidazole derivatives from simulations, including intraperturbed group contributions. These results are therefore derived from the differences in results of simulations of both the gas (ΔA_1) and aqueous phase (ΔA_2) paths. Table IIa presents results of free energy simulations in the gas phase and Table IIb in the aqueous phase. Table IIc presents the results for $\Delta\Delta A_{soln}$ obtained from differences between the aqueous and gas phase paths. The value of $\Delta\Delta A_{soln}$ for the transformation of 4-phenylimidazole to 1-phenylimidazole including only nonbonded intraperturbed group interactions is $+3.2 +/- 0.2$ kcal mol^{-1}; including all intraperturbed contributions for the same transformation, the value is $+2.6 \pm 0.2$ kcal mol^{-1}. These results bracket the value of $+3.0 \pm 0.02$ kcal mol^{-1} (SHAKE) obtained by neglecting all intraperturbed contributions. The results are comparable considering that they are barely outside the error limits for the values estimated from hysteresis, which are lower limits on the actual uncertainties. While the changes in vibrational terms make finite contributions to the accumulated free energies, their contribution is relatively small for the inhibitors which are the emphasis of this study. For all other transformation in Tables IIa, b, and c, only the nonbonded contributions to intraperturbed interactions were considered.

The result for the $\Delta\Delta A_{soln}$ for the transformation of 4-phenylimidazole to 3-methyl-4-phenylimidazole is 2.53 ± 0.3 kcal mol^{-1}, including intraperturbed nonbonded contributions, compared to 3.1 ± 0.3 kcal mol^{-1}, neglecting these contributions. The results for the difference in free energies of solvation between 2-PI and 4-PI including in-

TABLE II.
Results from Free Energy Simulations Including Intraperturbed Group Contributions.[a]

A. Gas Phase Calculation (ΔA_1 Cycle 2)

Inhibitor	Direction	ΔA_{gas}	ΔE_{gas}	$T(\Delta S_{gas})$
4-PI → 1-PI	Forward	+5.19	+5.19	−0.01
	Reverse	−5.21	−5.21	+0.01
4-PI → 1-PI[b]	Forward	+6.14	+6.14	0.00
	Reverse	−6.10	−6.11	−0.01
4-PI → 3-M4PI	Forward	4.01	3.73	−0.283
	Reverse	−3.84	−3.63	+0.213
2-PI → 4-PI	Forward	−2.04	−2.08	−0.03
	Reverse	+2.01	+2.08	+0.05
3M2PI → 2-PI	Forward	−30.99	−30.92	0.07
	Reverse	+31.72	+31.51	−0.21
2-PI → 1-PI	Forward	+2.50	+2.49	−0.01
	Reverse	−2.43	−2.43	−0.01

B. Solution Phase (ΔA_2 of Cycle 2)

Inhibitor	Direction	ΔA_{soln}	ΔE_{soln}	$T(\Delta S_{soln})$
4-PI → 1-PI	Forward	+8.28	7.58	−0.70
	Reverse	−8.54	−10.41	−1.88
4-PI → 1-PI[b]	Forward	+8.88	+7.19	−1.68
	Reverse	−8.54	−7.01	+1.54
4-PI → 3-M4PI	Forward	6.61	12.57	5.96
	Reverse	−6.30	−12.85	−6.55
2-PI → 4-PI	Forward	−2.31	0.66	2.97
	Reverse	2.37	−0.52	−2.89
3M2PI → 2-PI	Forward	+37.53	+35.37	−2.16
	Reverse	−38.06	−27.15	10.92
2-PI → 1-PI	Forward	+5.63	+0.38	−5.25
	Reverse	−6.20	−2.59	+3.61

C. Relative Free Energies of Solution Derived from Gas and Solution Phase Results ($\Delta\Delta A_{soln} = \Delta A_2 - \Delta A_1$)

Inhibitor	$\Delta\Delta A_{soln}$[c]	$\Delta\Delta E_{soln}$[c]	$T(\Delta\Delta S_{soln})$[c]
4-PI → 1-PI	+3.21 ± 0.2	+3.80 ± 2.0	*d*
4-PI → 1-PI[b]	+2.59 ± 0.2	+0.98 ± 0.3	−1.60 ± 0.1
4-PI → 3-M4PI	+2.53 ± 0.3	+9.03 ± 0.2	+6.01 ± 0.4
2-PI → 4-PI	−0.32 ± 0.04	+2.67 ± 0.0	+2.97 ± 0.1
3M2PI → 2-PI	+69.16 ± 0.6	+62.48 ± 5.8	−6.68 ± 6.2
2-PI → 1-PI	+3.46 ± 0.4	−0.98 ± 1.56	−4.44 ± 1.15

[a]All free energy results were obtained using free energy perturbation and SHAKE bond constraints, and were obtained under constant volume and temperature conditions. Only intraperturbed nonbonded interactions included, except where noted.
[b]All intraperturbed group contributions included.
[c]Values of thermodynamic quantities in this table were obtained by (1) obtaining the average forward direction quantities $\Delta\Delta A_{soln} = (1/2)\{[|\Delta A_f| + |\Delta A_r|]_{soln} - [|\Delta A_f| + |\Delta A_r|]_{gas}\}$, for example, for $\Delta\Delta A_{soln}$ and calculated analogously for the estimates of $\Delta\Delta E_{soln}$ and $T(\Delta\Delta S_{soln})$. The values are for the forward process as written in the column labeled Inhibitor. Uncertainties for $\Delta\Delta A_{soln}$ were estimated from the pooled standard deviations from the forward and reverse estimates from the solution and gas phase.
[d]The nature of the like signs for $T\Delta S$ for the aqueous path for the forward and reverse processes make this estimate particularly suspect. This simulation was the only simulation employing a 0.002-ps timestep in conjunction with 1000 steps of equilibration and 2000 steps of sampling per $\Delta\lambda$ window.

traperturbed nonbonded contributions are also seen to be similar to those obtained neglecting these contributions, shown in Table Ib. These results taken together indicate that for free energy changes dominated by changes in intermolecular nonbonded interactions, inclusion of intraperturbed group nonbonded contributions has modest effects.

In addition to these three free energies of solvation involving transformations of 4PI, Tables IIa, b, and c include two transformations to the 2PI isomer. The transformation of 3-methylammonium-2-phenylimidazole (3M2PI) to 2-phenylimidazole leads to $\Delta\Delta A_{soln} = +69.2 \pm 0.6$ kcal mol^{-1}, with the dominant contribution to the solvation free energy change due to the net change in charge. Table IIc also shows that the relative free energy of solvation of 2- and 1-phenylimidazole is $+3.4 \pm 0.3$ kcal mol^{-1}, comparable to the difference in solvation free energies between 4- and 1-phenylimidazole (3.2 ± 2 kcal mol^{-1}). The results of these two separate simulations are qualitatively consistent with one another in indicating a comparable magnitude difference in free energies of solvation between inhibitors possessing two distinct hydrogen bonding functional groups compared with 1-PI, which has but one such site. They differ quantitatively in that they jointly indicate a relative ordering of the magnitudes of the free energies of solvation of 2-PI and 4-PI (i.e., a difference of ca. $+0.2$ kcal mol^{-1}) opposite to the energy difference found by direct simulation of the relative free energies of solvation of 2-PI and 4-PI (i.e., -0.3 to -0.6 kcal mol^{-1}). Given the small difference in the free energy difference and the larger uncertainty in the value of $\Delta\Delta A_{soln}$(2-PI → 1-PI) than $\Delta\Delta A_{soln}$(4-PI → 1-PI), it is possible that $|\Delta\Delta A$(2-PI → 1-PI)$| < |\Delta\Delta A_{soln}$(4-PI → 1-PI)$|$ within the uncertainty in these predictions.

Tables Ia, Ib, and IIc include estimates of the differences in enthalpy $\Delta\Delta H_{soln}$, internal free energy $\Delta\Delta E_{soln}$, and $T(\Delta\Delta S_{soln})$ values. While the uncertainties in these separate components are expected to be at least an order magnitude greater than those for the $\Delta\Delta G_{soln}/\Delta\Delta A_{soln}$ values, the signs of the components provide additional insights into the differences in solvation of these analogs. The transformation of 4-phenylimidazole to 1-phenylimidazole results in $(\Delta\Delta S_{soln}) < 0$, obtained in both the constant pressure and constant volume simulations reported. This entropy difference is likely due to the greater ordering of the local solvent cage around the more hydrophobic 1-phenylimidazole. The $\Delta\Delta E_{soln}$ (or $\Delta\Delta H_{soln}$) > 0 for the transformation of 4- to 1-phenylimidazole in five of six independent simulations is consistent with the reduced electrostatic interaction of the 1-phenylimidazole with the waters of solvation compared to the 4-phenylimidazole, which can additionally act as a hydrogen bond donor to water.

TABLE III.
AMSOL-SM2 Results for Solvation Free Energies of Inhibitors of Cytochrome P450*cam* for AMSOL-Optimized and Nonoptimized (Frozen) Inhibitor Geometries.

Inhibitor	$\Delta G_{soln\text{-}opt}$	$\Delta G_{soln\text{-}frozen}$
1PI	−6.70	−7.02
4PI	−9.74	−9.86
2PI	−8.40	−8.10
3M4PI	−7.98	−8.18
3-M2PI	−71.22	−67.37

Tables III and IV present the estimates of solvation energies of each of the five inhibitors included in this study as determined from AMSOL-SM2 semiempirical quantum mechanical and Poisson-Boltzmann electrostatic calculations, respectively. The quantitative results for AMSOL-SM2 are very similar using optimized and frozen AMSOL geometries. This similarity is consistent with the observation that the AMSOL-SM2 optimized geometries were in fact very similar to the nonoptimized (frozen) AMSOL-SM2 geometries obtained from the 6-31G* optimized gas phase geometries with atomic root mean square (rms) deviations between them for 1PI of 0.10 Å, for 4-PI of 0.09 Å, for 2PI of 0.20 Å, for 3M4PI of 0.05 Å, and for 3M2PI of 0.6 Å. The deviations of the AMSOL gas phase geometries from the *ab initio* results were negligible (i.e., 0.01 Å). The frozen geometries used in the Poisson-Boltzmann calculations are the same as those used in the AMSOL-SM2 frozen geometry

TABLE IV.
ΔG_{soln}, Estimated from Poisson-Boltzmann Calculations.

Inhibitor	ΔG_{soln} (kcal mol^{-1})
1-PI	−10.24
4-PI	−12.31
2-PI	−10.41
3M4PI	−10.47
3M2PI	−57.56

TABLE V.
Comparison of $\Delta\Delta A_{soln}$ Estimates from Free Energy Simulation, AMSOL-SM2, and Poisson-Boltzmann Calculations.

Mutation	$\Delta\Delta A_{soln}$ FES[a]	AMSOL-SM2	Poisson-Boltzmann
4-PI → 1-PI	+3.21(no-intra) +2.59(intra-all) +3.21(intra-nonbond)	+3.04	2.07
4-PI → 3M4PI	+2.53(intra-nonbond) +3.0(no-intra)	+1.76	1.84
4-PI → 2-PI	+0.32(intra-nonbond) +0.63(no-intra)	+1.34	+1.90
2-PI → 3-M2PI	−69.16(intra-nonbond)	−62.82	−47.15
2-PI → 1-PI	+3.46(intra-nonbond)	1.70	+0.17

[a]The notation used in this column: (no-intra) means no intraperturbed group contributions were included; (intra-nonbond) indicates intraperturbed-nonbonded contributions were included, and (intra-all) refers to the case in which all intraperturbed group contributions were included in the free energy simulation results.

calculations. Thus, disparities between AMSOL and Poisson-Boltzmann calculations are not caused by geometry differences between the inhibitors.

Table V summarizes the free energy results obtained for the five inhibitors by the three different methods. As shown in this table, results from the free energy simulations and AMSOL methods are comparable, with the same rank order of the free energies of solvation of the five inhibitors 3M2-PI $\gg$ 4-PI > 2-PI > 3M4-PI > 1-PI for both free energy simulation and AMSOL results. Comparing the quantitative results for $\Delta\Delta A$, there is overall good agreement between the free energy simulations and AMSOL results, perhaps with the exception of the value for $\Delta\Delta A$(4-PI → 3M4-PI). The results for the Poisson-Boltzmann are not qualitatively comparable to those from either free energy simulations or AMSOL-SM2 calculations, with a different rank order of the differences for free energies of solvation of 3M2-PI > 4-PI > (3M4-PI $\approx$ 2-PI) > 1-PI, and different quantitative values for the differences in solvation free energies compared to the other two methods. The results indicate the inclusion of only electrostatic contributions, as found in the Poisson-Boltzmann formalism, to be insufficient to provide an accurate description of the relative free energies of solvation of the systems emphasized in this work. While one must be conservative in any interpretation of the differences in entropies of solvation derived from free energy simulations, it seems likely that it is the neglect of such terms in the Poisson-Boltzmann estimates which are largely responsible for the overall differences from the other two methodologies.

The underlying molecular basis for the trends in solvation free energies is traceable to the nature of the charge distribution, the nature of the polar interaction sites, and the consequent solution structure of the solvated inhibitors. Examination of molecular electrostatic potentials (not shown) for the 1-, 2-, and 4-phenylimidazoles outside their Connolly surfaces indicates regions of maximal electrostatic interactions with inhibitor polar atoms. Compared in this way, 2- and 4-phenylimidazole are very similar and have a region near the N1 atoms (cf. Fig. 1a) for interaction with water hydrogen atoms as well as a region near the N3—H3 group, indicating a potential for interaction with water oxygen atoms. In contrast to 2- and 4-PI, the 1-phenylimidazole potential surface indicates only one region of maximum electrostatic interaction (i.e., in the vicinity of the N3 atom). The lack of a second interaction site in 1-PI due to the absence of a second group capable of hydrogen bonding to the solvent is clearly the result of the inclusion of the N1 atom of 1-PI in the covalent linkage of the phenyl group.

Differences in the distribution of solvent atoms around the polar N and NH groups of the three inhibitors provide insight into the origin of their different free energies of solvation. Distribution functions for solvent atoms around the polar atoms of these inhibitors are shown in Figure 4. The N1 atom of 1PI does not have significant coordination

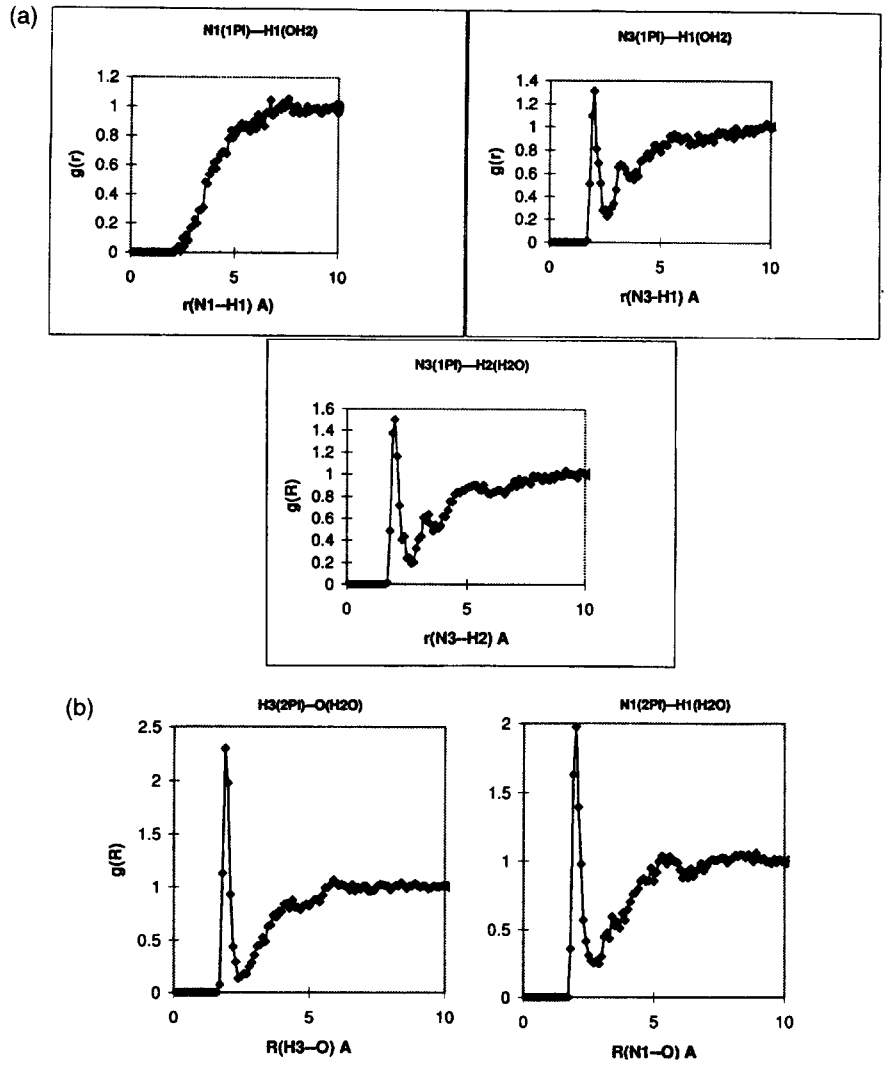

FIGURE 4. Inhibitor atom–water–atom radial distribution functions [$g(R)$'s] for (a) 1-PI, (b) 2-PI, and (c) 4-PI.

to water, as indicated by a lack of $g(R)$ values greater than unity (i.e., bulk water density) at short distances. This is a reasonable result given the covalent link of this nitrogen to the phenyl group at this position. However, the imidazole N3 of 1-PI is strongly coordinated to the two H atoms of water at a distance of 1.95 Å, with a probability of finding a solvent hydrogen at this distance greater than in bulk water. The coordination number of the N3 1-PI atom ($n = 4\pi \int_0^{r_{cut}} \rho g(R) r^2 \, dr$) deduced from integrating the distribution function to the minimum (r_{cut}) after the peak is a total of 1.9 water hydrogens. Figure 4b shows $g(R)$'s for 2-PI: for (water) hydrogens interacting with the N1 nitrogen (cf. Fig. 1) and water oxygens interacting with the H3 hydrogen attached to N3. Again, one notes clearly specific interactions between water and these atoms from the significant short distance peaks in the $g(R)$'s for this inhibitor. The coordination of the H3 atom to water oxygen atom from integrating the first peak in the (H3—O) $g(r)$ is 1.0, and the coordination number of the N1 atom for water hydrogens determined by integrating the peaks in the N1—H $g(R)$ is 1.3. Finally, Figure 4c shows the $g(R)$'s for polar atoms of 4-PI. Determination of the coordination numbers for water hydrogens close to the N1 atom gives a total of 2.0 and a total of 1.1 oxygens under the first peak in the H1—O distribution function.

While the extracted coordination numbers are approximate and cannot be straightforwardly equated with the equilibrium solvation thermodynamics, we see that the total number of specific hydrogen bonding interactions of inhibitor polar

atoms with water increases as follows: 1-PI(1.9) < 2-PI(2.3) < 4-PI(3.1). This order is precisely in accord with the results from the calculation of relative free energies of solvation and is clearly implicated as a determining factor in the solvation free energy trends observed.

Conclusions

The differences in free energies of solution for five phenylimidazoles have been computed by free energy simulations, continuum electrostatic Poisson-Boltzmann calculations, and semiempirical AMSOL-AM1-SM2 quantum mechanics calculations. The results of this study indicate the rank ordering of relative free energy differences, and the values obtained for the inhibitors studied determined from free energy simulations and AMSOL-SM2 are in agreement; while predictions made by Poisson-Boltzmann calculations are not in quantitative accord with predictions of the latter two methods. The better agreement of the predictions from free energy simulations with AMSOL-SM2 calculations than with estimates of relative solvation free energies from Poisson-Boltzmann calculations is not surprising considering that the latter theory only considers electrostatic energetics and completely lacks entropic terms clearly present in the underlying theory of the other two methods. The fairly good agreement between the AMSOL-SM2 and free energy simulation predictions for the five systems studied gives some credence to those predictions in the absence of experimental data for the free energies of solvation of these inhibitors.

Figure 5 shows three free energy cycles for the inhibitors with known P450*cam* binding affinities. Given for comparison are the differences in experimental binding free energies and calculated free energies of solvation for each of these inhibitors [i.e., value of $-\Delta G_2(\approx -\Delta\Delta A_2)$] determined in these studies. Note that the magnitude of the estimated difference in free energies of solvation $-\Delta G_2$ is nearly as large as the $\Delta\Delta G_{bind}$ for 4-PI and 2-PI relative to 1-PI. This correlation may imply that the predominant determinant for the differences in binding free energy of 1-PI versus either 2- or 4-PI is its lower free energy of desolvation upon binding to the enzyme, rather than preferential binding to the P450 site. While the noted correlation between relative solvation free energies and the experimental free energies does not preclude significant contributions to the computed relative free energies of binding of the inhibitors due to differences in the bound form of the inhibitors, it does indicate a trend consistent with the largely hydrophobic nature of the P450*cam*

(c)

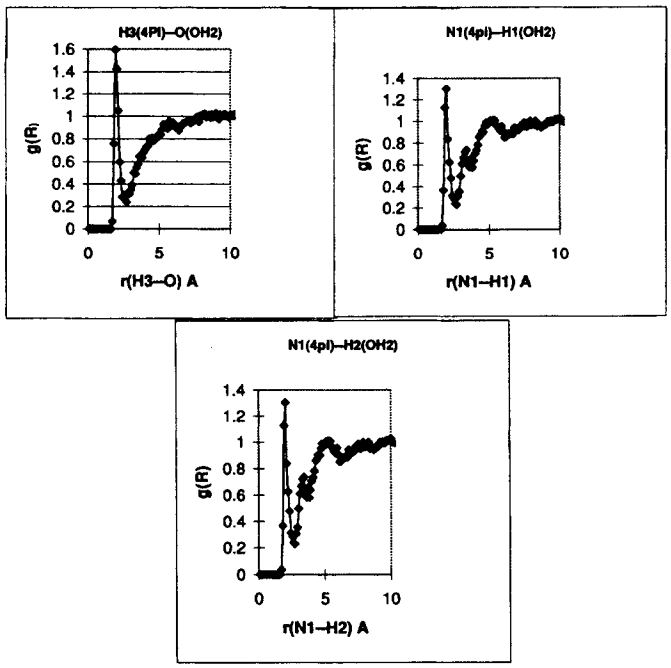

FIGURE 4—(*Continued*).

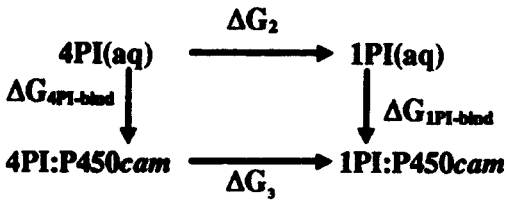

$\Delta\Delta Gbind = \Delta G_{1PI\text{-}bind} - \Delta G_{4PI\text{-}bind}$
$= \Delta G_3 - \Delta G_2 = -3.6$ kcal-mol^{-1}

$-\Delta G2 = -3.2$ kcal-mol^{-1}

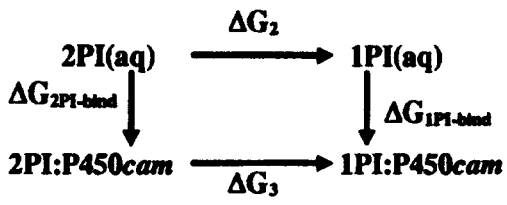

$\Delta\Delta Gbind = \Delta G_{1PI\text{-}bind} - \Delta G_{2PI\text{-}bind}$
$= \Delta G_3 - \Delta G_2 = -2.4$ kcal-mol^{-1}

$-\Delta G2 = ca. -3.4$ kcal-mol^{-1}

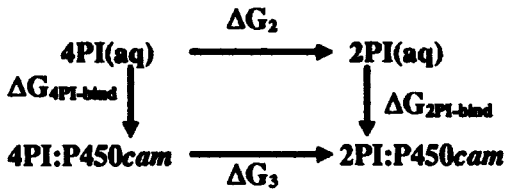

$\Delta\Delta Gbind = \Delta G_{2PI\text{-}bind} - \Delta G_{4PI\text{-}bind}$
$= \Delta G_3 - \Delta G_2 = -1.1$ kcal-mol^{-1}

$-\Delta G2 = -0.64$ kcal-mol^{-1}

FIGURE 5. Comparison of relative free energies of solvation with differences in experimental binding free energies and the relevant thermodynamic cycles.

active site (the relative importance of these two contributions is currently being checked by free energy simulations of the inhibitor bound forms of P450*cam*). The smaller free energy of solvation of the 1-PI compared to the 2-PI and 4-PI isomers is largely attributable to the lack of free N—H in the imidazole ring. This origin is confirmed by the finding of a similar difference in free energies of solvation in which a methyl group is added to the 3-position of the 4-PI isomer and of differences in equilibrium solvation distribution functions and coordination numbers for these derivatives.

The relatively good semiquantitative consistency of these results for inhibitors of cytochrome P450*cam*, the knowledge that the P450*cam* binding site is largely hydrophobic in character, and the parallel behavior of the relative magnitude of the predicted $\Delta\Delta G_{soln}$ and the known $\Delta\Delta G_{binding}$ indicate the plausibility of using comparisons of free energy of desolvation, calculated either by the free energy perturbation methods using constrained bond lengths and neglecting intraperturbed group approximations or by AMSOL methods, to screen candidate inhibitors and select favorable ones for further theoretical and experimental characterization in an effort to design inhibitors for P450*cam*.

Acknowledgments

The authors of this work would like to acknowledge support from NIH grant GM 27943 and an award of C-90 Supercomputer Service Units at the National Science Foundation (NSF)–sponsored Pittsburgh Supercomputing Center.

References

1. T. L. Poulos, B. C. Finzel, and A. J. Howard, *J. Biol. Chem.*, **195**, 687 (1987).
2. T. L. Poulos and A. J. Howard, *Biochemistry*, **26**, 8165 (1987).

3. J. D. Libscomb, *Biochemistry*, **19**, 3950 (1980).
4. D. L. Harris, Y.-T. Chang, and G. H. Loew, In *Modeling of Biomolecular Structures and Mechanisms*, A. Pullman, J. Jortner, and B. Pullman, Eds., Kluwer Academic Publishing, The Netherlands, 1995, p. 189.
5. P. Kollman, *Chem. Rev.*, **93**, 2395 (1993).
6. I. Alkorta, H. O. Villar, and J. J. Perez, *J. Comp. Chem.*, **14**, 620 (1993).
7. M. J. Frisch, G. W. Trucks, M. Head-Gordon, P. M. W. Gill, M. W. Wong, J. B. Foresman, B. G. Johnson, H. B. Schlegel, M. A. Robb, E. S. Replogle, R. Gomperts, J. L. Andres, K. Raghavachari, J. S. Binkley, C. Gonzalez, R. L. Martin, D. J. Fox, D. J. Defrees, J. Baker, J. J. P. Stewart, and J. A. Pople, Gaussian 92, Revision C, Gaussian, Inc., Pittsburgh, PA, 1992.
8. D. A. Pearlman, D. A. Case, J. C. Caldwell, G. L. Seibel, U. C. Singh, P. Weiner, and P. A. Kollman, AMBER UCSF Version 4.0, Department of Pharmaceutical Chemistry, University of California, San Francisco, 1986, 1991.
9. C. M. Breneman and K. W. Wiberg, *J. Comp. Chem.*, **11**, 361 (1990).
10. MSI/Quanta Version 3.3, Waltham, MA.
11. D. A. Pearlman and P. A. Kollman, *J. Chem. Phys.*, **94**, 4532 (1991).
12. Y. Sun, D. Spellmeyer, D. A. Pearlman, and P. A. Kollman, *J. Am. Chem. Soc.*, **114**, 6798 (1992).
13. D. A. Pearlman, *J. Chem. Phys.*, **98**, 8946 (1993).
14. L. Wang and J. Hermans, *J. Chem. Phys.*, **100**, 9129 (1994).
15. H.-A. Yu and M. Karplus, *J. Chem. Phys.*, **89**, 2366 (1988).
16. S. H. Fleischman and C. B. Brooks III, *J. Chem. Phys.*, **87**, 2460 (1987).
17. C. J. Cramer and D. G. Truhlar, *J. Comp.-Aided Molec. Design*, **6**, 629 (1992).
18. BIOSYM, Inc., San Diego, CA.